(2) Properties such as OACFs, correlation times, and spectral densities are easily calculated using λ_j's together with the weighting factor k_j's, which equally follow from the master equation but assume different values depending on the property investigated and the equilibrium statistics of the chain.

(3) Local chain dynamics is found to be significantly dependent upon the molecular structure, as the comparison of OACFs for PE and PEO in Figure 1 indicates.

(4) The present form of the dynamic RIS model which is developed for relatively short sequences in motion seems suitable for the interpretation of high-frequency motions of the order 10^{10}–10^{11}/s and, in particular, the spin–lattice relaxation and correlation times measured in NMR experiments with dilute polymeric solutions. The theory satisfactorily reproduces the experimentally measured spin–lattice relaxation and correlation times in ^1H and ^{13}C NMR, as well as the observed activation energies and the front factor, A_0. The agreement of the latter lends support to the postulated inverse linear dependence of A_0 on viscosity.

Acknowledgment. Financial support by NATO Grant 0321/87 is gratefully acknowledged. The authors thank Dr. F. Laupretre for useful discussions.

Registry No. PEO, 25322-68-3.

References and Notes

(1) Bahar, I.; Erman, B. *Macromolecules* **1987**, *20*, 1369.
(2) Bahar, I.; Erman, B. *Macromolecules* **1987**, *20*, 2310.
(3) Bahar, I.; Erman, B. *J. Chem. Phys.* **1988**, *88*, 1228.
(4) Bahar, I.; Erman, B.; Monnerie, L. *Macromolecules* **1989**, *22*, 431. Bahar, I.; Erman, B.; Monnerie, L. *Polym. Commun.* **1988**, *29*, 349.
(5) Jernigan, R. L. In *Dielectric Properties of Polymers*; Karasz, F. E., Ed.; Plenum: New York, 1972; p 99.
(6) Weber, T. A.; Helfand, E. *J. Phys. Chem.* **1983**, *87*, 2881.
(7) Hall, C.; Helfand, E. *J. Chem. Phys.* **1982**, *77*, 3275.
(8) Bendler, J. T.; Yaris, R. *Macromolecules*, **1978**, *11*, 650.
(9) Matsuo, K.; Stockmayer, W. H. *J. Phys. Chem.* **1983**, *87*, 2911.
(10) Liu, K. J.; Anderson, J. E. *Macromolecules* **1970**, *3*, 163.
(11) Hermann, G.; Weill, G. *Macromolecules* **1975**, *8*, 171.
(12) Lang, M.-C.; Laupretre, F.; Noel, C.; Monnerie, L. *J. Chem. Soc., Faraday Trans. 2* **1979**, *75*, 349.
(13) Heatley, F.; Walton, I. I. *Polymer* **1976**, *17*, 1019.
(14) Oppenheim, I.; Shuler, G. H.; Weiss, G. H. *Adv. Mol. Relax. Processes* **1967**, *1*, 13.
(15) Berne, B. J.; Pecora, R. *Dynamic Light Scattering*; Wiley: New York, 1976.
(16) Kramers, H. A. *Physica (Amsterdam)* **1940**, *7*, 284.
(17) Flory, P. J. *Statistical Mechanics of Chain Molecules*; Interscience: New York, 1969.
(18) Flory, P. J.; Mark, J. E. *Makromol. Chem.* **1964**, *75*, 11.
(19) Mark, J. E.; Flory, P. J. *J. Am. Chem. Soc.* **1966**, *87*, 1415.
(20) Mark, J. E.; Flory, P. J. *J. Am. Chem. Soc.* **1966**, *88*, 3702.
(21) Abe, A.; Kennedy, J. W.; Flory, P. J. *J. Polym. Sci., Polym. Phys. Ed.* **1976**, *14*, 1337.
(22) Abe, A.; Tasaki, K.; Mark, J. E. *Polym. J. (Tokyo)* **1985**, *17*, 883. Tasaki, K.; Abe, A. *Polym. J. (Tokyo)* **1985**, *17*, 641.
(23) Allerhand, A.; Doddrell, D.; Komoroski, R. J. *J. Chem. Phys.* **1971**, *55*, 189.
(24) Abragam, A. *Principles of Nuclear Magnetism*; Oxford University Press: London, 1961.
(25) Friedrich, C.; Laupretre, F.; Noel, C.; Monnerie, L. *Macromolecules* **1980**, *13*, 1625.
(26) Hermann, G. These d'Etat, Strasbourg, 1973 (from ref 25).
(27) Braun, D.; Tormala, P. *Makromol. Chem.* **1978**, *179*, 1025.

Polymeric Micelles: Their Relaxation Kinetics

A. Halperin*

The Fritz Haber Research Center for Molecular Dynamics, The Hebrew University, Jerusalem 91904, Israel, and Materials Department, University of California, Santa Barbara, California 93106

S. Alexander

Racah Institute of Physics, The Hebrew University, Jerusalem 91904, Israel.
Received July 27, 1988; Revised Manuscript Received October 19, 1988

ABSTRACT: Relaxation experiments—such as T jump—in solutions of polymeric micelles are theoretically analyzed. Only micelles formed by neutral A–B diblock copolymers in a selective solvent of low molecular weight are considered. The Aniansson–Wall mechanism, which allows the micellar size distribution to adjust in steps consisting of single-chain insertion/expulsion, is found to have the lowest activation free energy. The relaxation behavior is expected, as usual for micellar solutions, to be characterized by two relaxation times. The scaling form of the fast relaxation time, τ_1, is obtained by use of the properly adapted Kramers rate theory. τ_1 is found to have different forms for starlike micelles and for micelles with thin coronas. In both cases, $\tau_1 \sim \exp(N_B^{2/3}\gamma a^2/kT)$ where N_B is the core block's degree of polymerization (DP) and γ the surface tension of the core–corona interface. The preexponential factor is, however, different in the two systems. In solutions well past the critical micelle concentration (cmc), the preexponential factor scales as $N_B^{7/3}$ for micelles with thin coronas ($N_B \gg N_A$) and as $N_A^{9/5}N_B^{22/5}$ for starlike micelles ($N_B \ll N_A$) where N_A is the coronal block's DP. The different scaling laws are obtained because the passage through the corona is the rate-determining step only in starlike micelles.

I. Introduction

Much attention was given to the kinetics of micelle formation and dissolution.[1,2] Both experiment and theory focused on the response of micellar solutions to small perturbations, that is, relaxation experiments such as T jump. Most investigations dealt with the behavior of micelles formed by ordinary, small surfactants ($\sim C_{20}$). Very little, however, is known of the kinetics of polymeric micelles,[3] i.e., micelles formed by polymeric surfactants such as diblock copolymers. Studies of polymeric micelles, experimental[3,4] as well as theoretical,[5–11] considered their equilibrium properties. Yet, the kinetics of polymeric micelles should prove of interest both from polymer and

* Presently at The Hebrew University.

0024-9297/89/2222-2403$01.50/0

surface science points of view. Polymeric micelles provide an attractive model system for the study of micellar kinetics in general. Consider micelles formed by neutral diblock copolymers in a highly selective solvent. The behavior of this system is anticipated to be especially simple. This is because polymeric micelles are expected to grow or dissolve primarily via the Aniansson–Wall (AW)[2,12,13] mechanism. This mechanism allows change of the aggregation number only in steps consisting of addition or substraction of a single surfactant. For small surfactant micelles, the applicability of this model is limited by competing reactions involving fusion or fission of aggregates.[1,2,14] Polymeric micelles are distinct in that this last mechanism is expected to play only a minor role. Fusion of polymeric aggregates (micelles or "submicelles") is opposed by repulsive interactions due to the exterior coronal chains.[15] Also, the asymmetric, AW-type fission is favored by low activation free energies traceable to the core's surface free energy. Accordingly, the fission–fusion process should be very slow in comparison with the AW mechanism. Even more attractive is the option afforded by polymeric micelles to *modify rate constants with no accompanying change in the equilibrium properties relevant to the kinetics*, i.e., the aggregation number distribution. This option arises because the micellar size distribution is essentially independent of the coronal block's degree of polymerization (DP),[5,9,10] while the kinetics depend on the DP of the whole chain. Its realization depends on another feature inherent to polymeric surfactants: our ability to change the DP of either or both blocks over a wide range.

The kinetics of polymeric micelles are of interest not only as a simple model system. Relaxation experiments provide a simple probe of equilibrium properties to micellar solutions, such as the mean aggregation number and the variance of the aggregation number distribution. Furthermore, the study of the kinetics of polymeric micelles may shed light on their role in various applications. In particular, it may help to understand the kinetics of solubilization by such micelles, which are relevant to their use in dispersion polymerization and in the formulation of lubricants.[3] On a more fundamental level, the consideration of micellar kinetics involves questions concerning the desorption dynamics of polymeric surfactants. These are of interest because the polymers involved are *stretched*. In particular, the coronal blocks, which may be considered as grafted to the core's surface, are radially stretched. As a result[16] their outward motion is reptative in nature even in the absence of entanglements. Also, this motion is driven rather than purely diffusive. This is apparent upon realizing that each of the radially stretched coronal blocks is in effect confined to a cone (see section II). Their outward motion results then in release from confinement, and the associated loss of free energy drives the expulsion. These effects are discernible in the kinetics of starlike micelles. This feature is of interest from yet another point of view, as it is the origin of one of the uniquely polymeric modifications that is necessary for the application of the Kramers rate theory to our system.[17] Finally, this problem is of importance because similar considerations should apply to other related systems such as monolayers, lamellar phases, etc.

In the following we present theoretical considerations pertaining to relaxation experiments involving polymeric micelles formed by flexible, linear, neutral A–B diblock copolymers in a highly selective solvent. The copolymers are monodispersed, consisting each of N_A A monomers and N_B B monomers. While we focus on two limiting cases, of $N_A \ll N_B$ and $N_A \gg N_B$, both N_A and N_B are assumed to be large. The solvent, of low molecular weight, is assumed to be good for the A blocks and poor for the B blocks. As is usual for micellar solutions in general, we expect this system to exhibit two relaxation times, $\tau_1 \ll \tau_2$. We obtain the scaling behavior of shorter relaxation times, τ_1, with respect to N_A and N_B. The relaxation times depend on equilibrium properties, such as the mean and the variance of the aggregation number distribution, and on the rate constants for expulsion of a copolymer chain from a micelle. In section II we mainly review the equilibrium properties of polymer micelles. A plausibility argument for the dominance of the AW mechanism in our system is presented in section III. It is based on the comparison of the activation free energies associated with the two mechanisms. Accordingly, it is suggested that τ_2 of this system follows the predictions of the AW theory. While this argument is valid for τ_1 as well, it is of less consequence in this case as τ_1 is anyhow expected to have the AW form whenever the micellar size distribution is narrow enough. A brief review of the main predictions of the AW theory concludes this section. We do not attempt to obtain the scaling behavior of τ_2. This is because τ_2 depends on the expulsion rate constants and the concentrations of all the aggregates in the solution, while our aggregate's model is reasonable only for high aggregation numbers. We accordingly confine our considerations to the scaling behavior of τ_1. The dynamic property relevant to the analysis of τ_1 is the expulsion rate constant, b, for proper micelles. In section IV we present a scaling analysis of b within the framework of the Kramers rate theory. We then use it to obtain the scaling form of τ_1 for micelles with both thin and extended coronas. As is customary for scaling arguments, we usually ignore numerical prefactors.

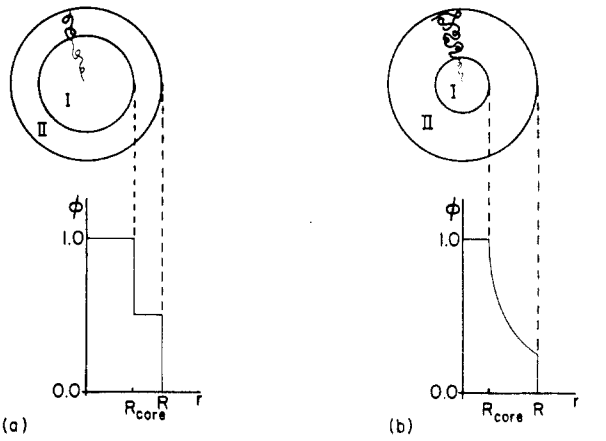

Figure 1. Two extreme micellar types: micelles with thin coronas (a) and starlike micelles (b). Schematic cross sections and plots of monomer volume fraction (Φ) versus the distance from the micelle center (r). Region I is a core consisting of a melt of B blocks. Region II is a corona of swollen A blocks. $\Phi(r)$ of micelles with thin coronas is depicted according to the Alexander–de Gennes model.

II. Polymeric Micelles

Diblock copolymers in a selective solvent form spherical micelles. Two spherical concentric regions are distinguishable in such a micelle: a central core consisting mostly of B blocks which are immiscible in the solvent, and an outer corona formed by soluble A blocks swollen by the solvent. It is possible to discern two extreme micellar types (Figure 1): micelles with thin dense coronas[5] ($N_A \ll N_B$) as opposed to starlike micelles with extended coronas[10] ($N_A \gg N_B$). The two types differ in their equilibrium properties and, as we shall see, in their dynamical behavior. It is convenient to consider dilute micellar solution well past

the critical micelle concentration (cmc). In this regime, the micelle's structure is essentially determined by the *free energy per chain of a single micelle.*

In a highly selective solvent, the only case we consider, the core–corona boundary, is sharply defined. The system's tendency to lower the associated surface free energy per chain, $F_{interface}$, drives the formation of micelles. Assuming that the core consists of closely packed B monomers, we have $V_{core} \approx {R_{core}}^3 \approx fN_Ba^3$, where f denotes the number of copolymer chains in a micelle and a is a typical monomer size. $F_{interface}$ is then given by[5]

$$F_{interface} \approx \gamma {R_{core}}^2/f \approx \gamma a^2 f^{-1/3} N_B^{2/3} \qquad \text{(II-1)}$$

The micelle's size is determined by the balance of $F_{interface}$ and free-energy penalties arising from micellar growth. These penalties originate from the localization of the A–B junction at the core–corona boundary. As a result, both core and coronal blocks are in effect grafted chains, i.e., chains attached to an interface by a headgroup. The coronal blocks are grafted to the exterior of the core, while the core blocks are attached to the core's inner surface. The high-density grafting causes chain deformation leading to an increased free energy which, in turn, arrests the micellar growth. We consider the contribution of the B blocks first.

For high enough temperatures, above the glass transition temperature, the inner core may be regarded as a melt of B blocks. The B chains are then assumed to obey ideal chain statistics. However, because of the grafting, the constant density ($\phi_B \approx 1$) requires chain stretching. Due to the core spherical symmetry, only some of the chains are stretched. Because of the steep decrease in available volume near the origin, it is sufficient to deform only some of the chains in order to fulfill the $\phi_B \approx 1$ constraint. Yet, it is possible to write the resulting increase in free energy per chain as

$$F_{core}/kT \approx {R_{core}}^2/{R_o}^2 \approx f^{2/3} N_B^{-1/3} \qquad \text{(II-2)}$$

where $R_o \approx N_B^{1/2} a$. While this form was originally justified by assuming uniform stretching,[5] subsequent analysis showed that (II-2) is obtained even when this assumption is relaxed.[18]

As noted earlier, coronal blocks are in effect grafted to the outer surface of the core. The high grafting density results in chain stretching and thus leads to the second penalty term, F_{corona}. To obtain F_{corona}, we utilize the scaling analysis, due to Witten and Pincus,[15] of chains grafted to a colloidal particle (in our case, the core). This approach is based on the Daoud–Cotton model for star polymers.[19] It is founded on two postulates: (1) The correlation length, ξ, depends only on r, the distance from the origin. Accordingly, the concentration profile is self-similar and $\xi \sim r$. (2) The correlation length in each spherical shell of radius r obeys $r^2 \approx f\xi^2$. In essence, the corona is divided into f identical truncated cones, and a coronal chain is grafted to the narrow end of each. The two postulates lead to $\xi \approx r/f^{1/2}$. Accordingly, the A monomers' volume fraction in a good solvent is given by $\phi_A(r) \approx f^{2/3}(a/r)^{4/3}$. By integrating $\phi_A(r)$ over the coronal volume and setting the integral equal to $N_A f a^3$, we obtain the thickness of the corona, L:

$$L \approx \begin{cases} f^{1/9} N_B^{-2/9} N_A a & N_A \ll N_B \\ f^{1/5} N_A^{3/5} a & N_A \gg N_B \end{cases} \qquad \text{(II-3)}$$

The associated free energy per chain is obtainable by integrating the free-energy density[11] given by kT/ξ^3 or equivalent by the kT per blob recipe:[15]

$$F_{corona}/kT \approx f^{-1} \int_{R_{core}}^{R_{core}+L} \xi^{-3} r^2 \, dr \approx f^{1/2} \ln (1 + L/R_{core}) \qquad \text{(II-4)}$$

and thus

$$F_{corona}/kT \approx \begin{cases} f^{1/2}(L/R_{core}) \approx f^{5/18} N_B^{-5/9} N_A & N_A \ll N_B \\ f^{1/2} \ln (L/R_{core}) \sim f^{1/2} \ln (f^{-2/15} N_B^{-1/3} N_A^{3/5}) & N_A \gg N_B \end{cases} \qquad \text{(II-5)}$$

In the limit $N_A \ll N_B$, (II-3) and (II-5) yield the forms obtained for flat grafted layers;[5,20,21] however, the average separation of grafting sites is now self-adjusting. In this treatment, the coronal chains are taken to be uniformly stretched. As in the case of the core, this assumption is questionable. A self-consistent analysis of spherical grafted layers has yet to be performed. However, a recent self-consistent calculation[22] shows that the scaling behavior of L and F_{corona} in the case of a flat grafted layer ($N_A \ll N_B$) does not change when the uniform stretching constraint is relaxed.

We now approximate the free energy per chain in a single micelle as

$$F_{micelle} = F_{interface} + F_{core} + F_{corona} \qquad \text{(II-6)}$$

In doing so we neglect minor corrections such as those due to the junctions' entropy, their localization at the interface, and the bonding of pairs of core and coronal blocks. In the two limits of interest, further simplifications are possible: For micelles with thin coronas, ($N_A \ll N_B^{11/18}$)$F_{corona} \ll F_{core}$, while for starlike micelles, ($N_A \gg N_B^{11/15}$)$F_{corona} \gg F_{core}$. Accordingly,[5,10,11]

$$F_{micelle}/kT \approx \begin{cases} (\gamma a^2/kT) f^{-1/3} N_B^{2/3} + f^{2/3} N_B^{-1/3} & N_A \ll N_B^{11/18} \\ (\gamma a^2/kT) f^{-1/3} N_B^{2/3} + f^{1/2} & N_A \gg N_B^{11/15} \end{cases} \qquad \text{(II-7)}$$

where the logarithmic factor due to F_{corona} was taken for a constant. In other words, the micellar growth is checked by F_{corona} for starlike micelles and by F_{core} for micelles with thin corona. Upon minimizing $F_{micelle}$ with respect to f, we obtain the scaling behavior of the mean aggregation number[5,10,11]

$$\langle f \rangle \sim \begin{cases} N_B & N_A \ll N_B^{11/18} \\ N_B^{4/5} & N_A \gg N_B^{11/15} \end{cases} \qquad \text{(II-8)}$$

As ${R_{core}}^3 \approx fN_Ba^3$, this leads to

$$\langle R_{core} \rangle \sim \begin{cases} N_B^{2/3} a & N_A \ll N_B^{11/18} \\ N_B^{3/5} a & N_A \gg N_B^{11/15} \end{cases} \qquad \text{(II-9)}$$

and to

$$\langle R \rangle \approx \begin{cases} \langle R_{core} \rangle \sim N_B^{2/3} a & N_A \ll N_B^{11/18} \\ \langle L \rangle \sim N_B^{4/25} N_A^{3/5} a & N_A \gg N_B^{11/15} \end{cases} \qquad \text{(II-10)}$$

where $\langle R \rangle$ denotes the average overall radius of a micelle. Thus, the size of a starlike micelle is set by the corona, while the dimensions of micelles with thin coronas are determined by the core. The variance, σ^2, of the aggregation number distribution is the last equilibrium property needed. Following Leibler et al.,[7] we obtain a rough es-

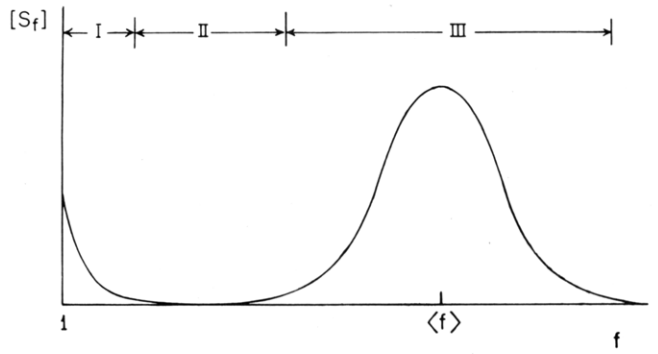

Figure 2. Schematic aggregate size distribution characteristic of micellar solutions: $[S_f]$, the concentration of aggregates consisting of f surfactants versus the aggregation number, f.

timate of σ^2 by considering Gaussian fluctuations around $\langle f \rangle$. Accordingly,

$$\sigma^2 \approx kT/\langle f \rangle F''_{\text{micelle}}(\langle f \rangle) \qquad \text{(II-11)}$$

where $F'' = \partial^2 F/\partial f^2$. The scaling behavior of the standard deviation, σ, is then as follows:

$$\sigma \sim \begin{cases} N_B^{1/3} & N_A \ll N_B^{11/18} \\ N_B^{1/5} & N_A \gg N_B^{11/15} \end{cases} \qquad \text{(II-12)}$$

III. Relaxation Kinetics of Micellar Solutions[1,2,14]

The relaxation of micellar solutions following a small perturbation is characterized by two relaxation times, τ_1 and τ_2, such that $\tau_1 \ll \tau_2$. In essence, this is due to the bimodal size distribution typical of micellar solutions past the cmc (Figure 2). The concentrations of unaggregated surfactants (zone I) and of proper micelles (zone III) are comparatively high, while intermediate-sized aggregates (submicelles) are present in very low concentrations (zone II). The fast relaxation processes are associated with reactions involving abundant species, while the slow process is said to involve scarce submicellar aggregates (zone II). In particular, the slow relaxation process is attributed to reactions leading to a change in the total number of micelles, i.e., formation or dissolution of micelles. The fast process is ascribed to reactions resulting in redistribution of micellar sizes with no accompanying change in their total number. The precise form of τ_2 depends on the postulated mechanism. Two mechanisms are considered to be involved: (1) The AW mechanism excludes reactions between aggregates. Only reactions involving aggregates and nonaggregated surfactants are allowed:

$$S_i + S \underset{b_{i+1}}{\overset{a_{i+1}}{\rightleftharpoons}} S_{i+1} \qquad \text{(III-1)}$$

(2) The second mechanism allows relaxation by fission or fusion of aggregates:

$$S_i + S_j \rightleftharpoons S_{i+j} \qquad \text{(III-2)}$$

The two mechanisms lead to markedly different functional forms for τ_2. The first mechanism predicts τ_2 to be an increasing function of the micelles' concentration, while the second one leads to τ_2 which decreases with the concentration but levels off for high enough concentrations. The concentration dependence of τ_2 in the AW scheme arises because it characterizes flux through a "bottleneck" (zone II). The opposite trend, found for the fission–fusion mechanism, is typical of the second-order kinetics associated with aggregate–aggregate collisions. While the involvement of the fission–fusion mechanism has a marked effect on τ_2, τ_1 is determined primarily by the AW scheme. This is because the fission–fusion mechanism is not efficient in achieving slight readjustments of the sharply peaked micellar distribution (zone III). Experimental evidence indicates that the relaxation of nonionic systems is dominated by the fission–fusion mechanism from the cmc onwards. Ionic micelles are thought to follow the AW mechanism in low and intermediate ionic strength solutions, but the fission–fusion mechanism takes over for high ionic strength. Micelle–micelle interactions seem to determine the dominant relaxation mechanism. Repulsive interactions between micelles tend to favor the AW mechanism. For ordinary micelles, such interactions are due to electrostatic repulsion. While polymeric micelles are the macromolecular counterpart of ordinary nonionic micelles, their relaxation behavior is expected to be markedly different. Neutral polymeric micelles formed by diblock copolymers repel each other because of the steric interactions between the coronas. Accordingly, neutral polymeric micelles, as opposed to their "small surfactant" counterpart, are expected to relax via the AW mechanism.

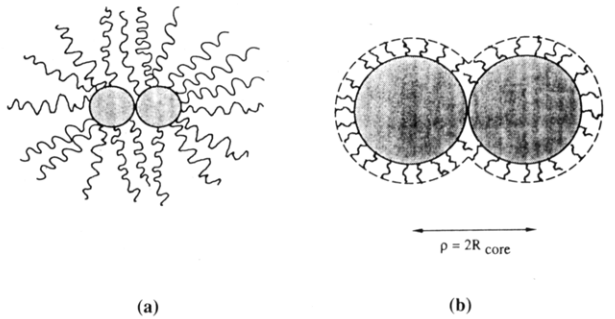

Figure 3. Schematic cross sections of reactive intermediates involving (a) starlike aggregates and (b) aggregates with thin coronas. The intermediates shown are obtained for the fission–fusion mechanism.

It is possible to present a detailed argument favoring the AW mechanism for polymeric micelles. The argument is based on an identification of the intermediate state, "activated state" of the two mechanisms. The associated activated energies are then clearly seen to favor the AW scheme. The intermediate state consists of two aggregates (micelles or submicelles) in close proximity such that the cores are in grazing contact and the coronas are partly overlapping (Figure 3). When the two aggregates consist each of a number of chains, the intermediate corresponds to the fission–fusion mechanism. In the limiting case where one of the aggregates consists of a single diblock copolymer, the intermediate belongs in the AW scheme. In the latter case, the core of the aggregate is adjacent to the collapsed B block of the diblock copolymer. To make our point, we must obtain the activation free energies associated with the fission and fusion processes (expulsion and insertion in the AW scheme) for the two kinds of micelles under consideration. The fission activation free energy, $\delta\Phi_{\text{fission}}$, is simpler to obtain. This is because the coronal contribution to $\delta\Phi_{\text{fission}}$ is negligible in the two cases we consider. For micelles with thin coronas, the coronal contribution to $\delta\Phi_{\text{fission}}$ is by definition negligible in comparison with $F_{\text{interface}}$ and F_{core}. In the case of starlike micelles, the coronal structure is only slightly perturbed by rearrangement of the core blocks and F_{corona} is roughly constant. Consider then the fission of an aggregate consistng of f chains into an intermediate composed of two parts consisting of f_1 and f_2 chains ($f_1 + f_2 = f$). As usual, $\delta\Phi_{\text{fission}}$ is given by

$$\delta\Phi_{\text{fission}} = \Phi(f_1) + \Phi(f_2) - \Phi(f) \qquad \text{(III-3)}$$

where, for fission, $\Phi(f)$ is given by

$$\Phi(f)/f = F_{core} + F_{interface} \quad \text{(III-4)}$$

Note again the absence of coronal contribution. Here, as opposed to the discussion in section II, the free energy per aggregate is important. To allow us to treat collapsed coils, F_{core}, as given in (II-2), is now supplemented by the kT ln (R_{core}/R_o) term. To ensure positive $\delta\Phi_{fission}$ for $f = \langle f \rangle$, numerical prefactors must be included. Thus, because $V_{core} = fN_Ba^3 = (4/3)\pi R_{core}^3$, the core surface area in $F_{interface}$ is equal to $4\pi R_{core}^2 = (4\pi)^{2/3}3^{2/3}f^{2/3}N_B^{2/3}a^2 \approx 4.8f^{2/3}N_B^{2/3}a^2$. Because the core chains are stretched one dimensionally, a $^1/_2$ factor should multiply the augmented F_{core}. Altogether we obtain

$$\frac{1}{kT}\delta\Phi_{fission} = (4\pi)^{1/3}3^{2/3}f^{2/3}N_B^{2/3}\frac{\gamma a^2}{kT}[x^{2/3} + (1-x)^{2/3} - 1] + \frac{1}{2}f^{5/3}N_B^{-1/3}[x^{5/3} + (1-x)^{5/3} - 1] - \frac{1}{6}f[x \ln x + (1-x)\ln(1-x)] \quad \text{(III-5)}$$

where $x = f_1/f$. The first term accounts for the surface free-energy contribution to $\delta\Phi_{fission}$, while the two following terms allow for the elastic free energy of the core B blocks. Of the three terms, only the middle one is negative. $\delta\Phi_{fissio(}$ is symmetric with respect to an extremum at $x = {}^1/_2$ and it vanishes at $x = 1$ and $x = 0$. It is positive for all f's smaller than $\langle f \rangle$. (It can change sign only for f values which are approximately twice larger than $\langle f \rangle$ of a micelle with thin corona.) For small x values, $\delta\Phi_{fission}/kT \sim f^{2/3}N_B^{2/3}x^{2/3}$. As x can only assume values that are integer multiples at f^{-1}, i.e., $x = if^{-1}$, we have $\delta\Phi_{fission}/kT \sim N_B^{2/3}i^{2/3}$, which clearly favors the AW mechanism ($i = 1$).

The activation free energy associated with fusion or insertion processes, $\delta\Phi_{fusion}$, is primarily due to coronal interactions. $\delta\Phi_{fusion}$ for the formation of an intermediate by fusion of two aggregates consisting of f_1 and f_2 coils is given by

$$\delta\Phi_{fusion} = (f_1 + f_2)F_{corona}(f_1 + f_2) - f_1F_{corona}(f_1) - f_2F_{corona}(f_2) \quad \text{(III-6)}$$

where $F_{corona}(f_1 + f_2)$ refers to the free energy per chain of the intermediate. The form of $\delta\Phi_{fusion}$ for starlike micelles is different from that obtained for micelles with thin coronas. For starlike micelles, $F_{corona}(f_1 + f_2)$ is roughly that of $f_1 + f_2 = f$ A coils grafted to the bigger of the two cores. As before, we approximate the logarithmic factor in (II-5) as a constant of order unity, thus leading to

$$\frac{1}{kT}\delta\Phi_{fusion} \sim (f_1 + f_2)^{3/2} - f_1^{3/2} - f_2^{3/2} \sim \begin{cases} f^{3/2} & f_1 \approx f_2 \approx f/2 \\ f_1f^{1/2} & f_1 \ll f_2 \approx f \end{cases} \quad N_A \gg N_B \quad \text{(III-7)}$$

Equation III-7 is only valid for large enough f's such that it is legitimate to consider the corona as starlike. For the same reason, (III-7) applies only to f_1's which are sufficiently large (≥7). With regard to this last caveat, it turns out however that the same form is obtained even for the insertion of few chains, i.e., $f_1 = 1$, 2, etc. The activation energy associated with the AW insertion process is thus lowest, and accordingly this should be the favored mechanism for the relaxation of starlike micelles. Our analysis of $\delta\Phi_{fusion}$ of starlike micelles relied on the approximate spherical symmetry of the activated complex corona. For activated states involving micelles with thin coronas, this approximation is not always valid. In particular, the corona of an intermediate state associated with the fusion of similarly sized aggregates is not spherical in shape. In such cases, the detailed geometry of the complex should be taken into account along the lines suggested by Leibler and Pincus.[23] The intermediate's corona is depicted as two partly overlapping spherical shells (Figure 3). For two identical aggregates with grazing cores, that is when the distance between their centes ρ is $2R_{core}$, the coronal volume is

$$V_{corona}(\rho = 2R_{core}) = \frac{4\pi}{3}R_{core}^3\left(6z + \frac{9}{2}z^2 + z^3\right) \quad \text{(III-8)}$$

where $z = L/R_{core}$. In these terms, the coronal volume of two nonoverlapping aggregates, i.e., $\rho = 2R_{core} + 2L$, is given by

$$V_{corona}(\rho = 2R_{core} + 2L) = \frac{4\pi}{3}R_{core}^3(6z + 6z^2 + 2z^3) \quad \text{(III-9)}$$

Note that in general L in the two cases is different. The Flory-type mean field coronal free energy, $\tilde{\Phi}_{corona}$, is then

$$\frac{1}{kT}\tilde{\Phi}_{corona} \approx 2f\left(\frac{L^2}{N_Aa^2} + \upsilon\frac{4f^2N_A^2}{V_{corona}}\right) \quad \text{(III-10)}$$

where υ is the second virial coefficient for the coronal blocks. The corresponding activation free energy within this picture is

$$\delta\Phi_{fusion} = \tilde{\Phi}_{corona}(\rho = 2R_{core}) - \tilde{\Phi}_{corona}(\rho = 2R_{core} + 2L) \quad \text{(III-11)}$$

In the limit of interest, of micelles with thin coronas, $z \ll 1$, L does not change significantly with coronal overlap. As a result,

$$\frac{1}{kT}\delta\Phi_{fusion} \approx \upsilon f^3N_A^2[V_{corona}^{-1}(\rho = 2R_{core}) - V_{corona}^{-1}(\rho = 2R_{core} + 2L)] \quad \text{(III-12)}$$

which, to leading order in z, yields

$$\frac{1}{kT}\delta\Phi_{fusion} \approx \frac{\upsilon}{a^3}f^2\frac{N_A^2}{N_B} \quad \text{(III-13)}$$

A rough estimate of $\delta\Phi_{fusio(}$ associated with the AW process is given by

$$\delta\Phi_{fusion} \approx \tilde{\Phi}(f+1) - \tilde{\Phi}(f) \quad \text{(III-14)}$$

where $\tilde{\Phi}$ is given by (III-10) except that f replaces $2f$ in $\tilde{\Phi}(f)$. As L is only weakly dependent on f, we disregard a slight increase in L upon insertion of the extra coil. For $f \gg 1$, we obtain

$$\frac{1}{kT}\delta\Phi_{fusion} \approx \frac{L^2}{N_Aa^2} + \frac{\upsilon}{a^3}\frac{N_A^2f}{V_{corona}} \sim f^{2/9}N_B^{-4/9}N_A \quad \text{(III-15)}$$

where we have approximated V_{corona} as $V_{corona} \approx R_{core}^2L$. Scaling analysis yields a slightly different form for (III-15): $\delta\Phi_{fusion}/kT \sim f^{5/18}N_B^{-5/9}N_A$. The trend is, however, clear: The activation energy associated with the AW process is lowest, and accordingly this mechanism is expected to be dominant. While this trend is found for all cases considered, our analysis may only serve as a plausibility argument. A rigorous theory requires complete knowledge of concentrations and rate constants of all aggregates. Such analysis is beyond the scope of this paper.

We conclude this section with a brief review of the AW theory. The relevant results for a micellar solution relaxing by the AW mechanism are as follows.[2,12,13] The fast process is characterized by the relaxation time, τ_1, given by

$$\frac{1}{\tau_1} = \frac{b}{\sigma^2} + \frac{b}{\langle f \rangle}X(1 + C_o) \approx \frac{b}{\sigma^2}\left(1 + \frac{\sigma^2}{\langle f \rangle}X\right) \quad \text{(III-16)}$$

b is the expulsion rate constant for proper micelles, which is assumed to be identical for all micelles in zone III. X is a dimensionless concentration defined by

$$X = \frac{[S_{total}] - [S]}{[S]} \quad \text{(III-17)}$$

where $[S_{total}]$ is the total surfactant concentration in the system and [S] is the equilibrium concentration of unaggregated surfactants, which is essentially identical with the cmc. C_0 is the average relative deviation from equilibrium in the system. For relaxation experiments, C_0 is negligibly small compared to unity. The relaxation time characteristic of the slow process is given by

$$\frac{1}{\tau_2} \approx \frac{\langle f \rangle^2}{[S]} \frac{1}{R}\left(1 + \frac{\sigma^2}{\langle f \rangle} X\right)^{-1} \quad \text{(III-18)}$$

where

$$R = \sum_{f \in II} \frac{1}{b_f [S_f]} \quad \text{(III-19)}$$

$[S_f]$'s are the equilibrium concentrations of aggregates consisting of f surfactants and b_f the corresponding expulsion rate constants. The derivation of (III-16) and (III-18) is based on two important assumptions: The deviations from equilibrium are assumed to be small. This allows us to take the equilibrium size distribution (Figure 2) as essentially correct. The second assumption is that $\tau_2 \gg \tau_1$, i.e., that the fast process is to all intents completed before the slow process advances to a significant degree. The existence of two disparate time scales amounts to decoupling of the two processes. As a result, we may take the total number of micelles to be constant while the fast process is under way. To obtain τ_2, a stationary state assumption was made with regard to all species in zone II. Other, less fundamental assumptions were made in order to obtain an expression for τ_1. The aggregation number distribution of various species in zone III was assumed to be Gaussian. The expulsion rate constants, b_f, in zone III are taken to be independent of f. And, finally, the $[S_f]$'s in zone III are assumed to behave as continuous and differentiable functions of the aggregation number, f. Our discussion suggests that solutions of polymeric micelles relax via the AW mechanism. Their relaxation behavior should then be characteized by τ_1 and τ_2, respectively, given by (III-16) and (III-18). We will not attempt to elaborate further on our prediction with regard to τ_2. Rather, we focus on the scaling behavior of τ_1.

IV. The Expulsion Rate Constant

Thus far we have compared the activation energies associated with two possible relaxation mechanisms of polymeric micelles. This comparison suggests that the AW mechanism should dominant the relaxation of micelles formed by diblock copolymers. By extending these considerations, it is possible to suggest a scaling form for b, the expulsion rate constant characteristic of proper micelles (zone III). This, together with the scaling laws for σ^2 and $\langle f \rangle$ ((II-8) and (II-12)), should then yield the scaling behavior of τ_1. An intermediate state was assumed to play a role in the expulsion of a coil out of micelle. This suggests the use of transition state theory[24] or one of its derivatives to obtain b. In this case, because we are dealing with a classical system in which viscosity plays an important role, the Kramers theory[25,26] provides an appropriate framework. We will first review the pertinent aspects of this theory and then modify it to allow for the special features of our system. Because we consider macromolecules in a meltlike core medium, we focus on the high viscosity limit of this theory. Consider then an ensemble of noninteracting particles which are trapped in a potential well (Figure 4). Initially all particles are trapped, but in time, a growing number escapes the well. Their outward motion is assumed to be diffusive, i.e., follow the Smoluchowski equation. For one-dimensional stationary flow along the "reaction coordinate", y, the diffusion current, J, may be written as

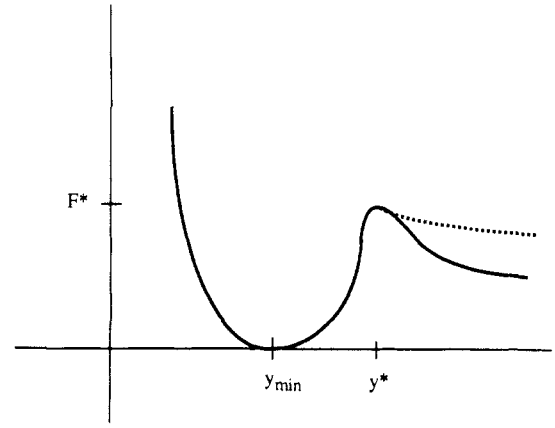

Figure 4. Schematic free-energy profile considered in the Kramers rate theory. The dotted line denotes the beginning of the long ranged potential tail experienced by diblock copolymer coils while expelled through the micellar corona.

$$J = -D \exp(-F/kT) \frac{\partial}{\partial y} c \exp(F/kT) \quad \text{(IV-1)}$$

where $c(y)$ denotes the local concentration of the diffusing particles and $F(y)$ the free energy profile of the well. Because J is a constant, integration over y between the well minimum and the bulk yields

$$J = -\frac{Dc \exp(F/kT)\Big|_{y_{min}}^{y_{bulk}}}{\int_{y_{min}}^{y_{bulk}} \exp(F/kT)\, dy} \quad \text{(IV-2)}$$

For our choice of reference state, $F(y_{min}) = 0$, and as $c(y_{bulk}) \approx 0$, the numerator is equal to $Dc(y_{min})$. To evaluate the denominator, we expand $F(y)$ around its maximum, $F(y^*) = F^*$ to second order in $y - y^*$: $F(y) \approx F^* - {}^1/_2 w(y - y^*)^2$. We then obtain a Gaussian integral yielding $(2\pi kT/w)^{1/2} \exp(F^*/kT)$ for the denominator. Altogether J is now given by

$$J \sim \frac{Dc(y_{min}) e^{-F^*/kT}}{(2\pi kT/w)^{1/2}} \quad \text{(IV-3)}$$

Note that the width of the barrier kT below F^*, α, is given by $kT/w \sim \alpha^2$. Accordingly, $D(2\pi kT/w)^{-1/2} \sim D\alpha^{-1} \sim \alpha \tau_{barrier}^{-1}$ where $\tau_{barrier} \sim D^{-1}\alpha^2$ is the time required by a particle to diffuse a distance α, i.e., across the top of the barrier. We may thus rewrite J as[17]

$$J \sim c(y_{min}) e^{-F^*/kT} \alpha \tau_{barrier}^{-1} \sim c(y^*) v_{barrier} \sim c(y_{min}) v_{diffusion} \quad \text{(IV-4)}$$

where $v_{barrier} \sim \alpha \tau_{barrier}^{-1}$ is the velocity of the diffusive current across the top of the barrier, $c(y^*) = c(y_{min}) e^{-F^*/kT}$ is the concentration of the reactive intermediate, and $v_{diffusion} = e^{-F^*/kT} v_{barrier}$ is the effective velocity of the diffusive current. The corresponding reaction rate may be written as a unimolecular rate equation $dc(y_{bulk})/dt = kc(y_{min})$. The unimolecular rate constant, k, is determined by the time, τ, characterizing the outward motion of the particles. Thus, if R is a characteristic dimension of the well, $\tau \sim R/v_{diffusion}$ and

$$k \sim \tau^{-1} \sim v_{\text{diffusion}}/R \qquad \text{(IV-5)}$$

It is convenient to summarize this discussion in terms of the following, standard, kinetic scheme:

$$A \underset{-1}{\overset{1}{\rightleftharpoons}} A^* \xrightarrow{2} \text{products} \qquad \text{(IV-6)}$$

The stationary flow assumption, J = constant', is equivalent to the stationary state assumption, $d[A^*]/dt = 0$, as used in chemical kinetics. Both transition state theory and the Kramers theory consider a slow (2) reaction such that a quasi-thermal equilibrium is established between A and A*, i.e., inside the well. Further, both theories identify the lifetime of A*, the reactive intermediate, with the time required to cross the top of the potential barrier. The two theories differ in the kind of motion invoked to achieve the crossing. In the transition state theory, the particles are assumed to have a non-zero average velocity,[24] $\langle \dot{y} \rangle \neq 0$, and accordingly $\tau_{\text{barrier}} \sim \alpha$. In the high viscosity limit of the Kramers theory $\langle \dot{y} \rangle = 0$, and the particle crosses the barrier by Brownian motion leading to $\tau_{\text{barrier}} \sim \alpha^2$. We will now adapt the Kramers theory in order to obtain the expulsion rate constant, b, for polymeric micelles. The escaping particles considered are now diblock copolymers. Two special features appear in this case: (i) The actual path traversed by the chain is sometimes much longer than the associated displacement along the reaction coordinate. As a result, τ_{barrier} is longer than expected. This effect is reminiscent of reptation. (ii) The velocity characterizing the passage of the particle from y^* into the bulk, v_{corona}, is in certain cases slower than v_{barrier}. In such cases, the passage through the corona becomes the rate-determining step and v_{corona} replaces v_{barrier} in the expressions for J and b. This effect arises because τ_{barrier} is determined primarily by the B block, while τ_{corona} is set by the A block.

We picture the expulsion as a two-stage process. Initially the B block is gradually ejected out of the core, forming a spherical "bud" of radius r_{bud}. The radius of the bud corresponds to that of a collapsed B coil consisting of the instantaneous number of ejected B monomers, i.e., $0 \leq r_{\text{bud}} \leq N_B^{1/3}a$. As long as the B block is partly embedded in the core, the A block is only slightly perturbed. This stage of the process is a highly asymmetric fission, but to avoid confusion, we will refer to it as "budding". Once the budding stage is completed, the expulsion of the entire diblock copolymer out of the corona can take place. This stage is dominated by the behavior of the A block with the collapsed B block contributing somewhat to the frictional characteristics of the process. We now identify the distance of the A–B junction from the micelle's center as the reaction coordinate, y. The well's minimum is thus located at $y_{\text{min}} = R_{\text{core}}$; the barrier's highest point, F^*, is found at $y^* \approx R_{\text{core}} + 2N_B^{1/3}a$; and the expulsion is completed when $y = y_{\text{bulk}} = R_{\text{core}} + L$. The budding process corresponds to the interval $R_{\text{core}} \leq y \approx R_{\text{core}} + 2r_{\text{bud}} \leq R_{\text{core}} + 2N_B^{1/3}a$, while the coronal stage takes place for $R_{\text{core}} + 2N_B^{1/3}a \leq y \leq R_{\text{core}} + L$. Knowledge of the free-energy profile, $F(y)$, especially in the vicinity of F^*, is a prerequisite for the application of the Kramers theory. $F(y)$ for the budding stage is dominated by F_{surface}. This is apparent from (III-5) for $\delta\Phi_{\text{fission}} = F^* - F(y_{\text{min}})$ which, for the AW process, is due primarily to the surface tension contribution. Accordingly, for $R_{\text{core}} \leq y \leq R_{\text{core}} + 2N_B^{1/3}a$, we have

$$F(y) \approx \gamma(r_{\text{bud}}^2 + R^2 - R_{\text{core}}^2) \approx \gamma r_{\text{bud}}^2 \qquad \text{(IV-7)}$$

where R is the instantaneous core radius corresponding to a given r_{bud} such that $R^3 + r_{\text{bud}}^3 = R_{\text{core}}^3$. Note that the bottom of the well serves as a reference state; i.e., $F(y_{\text{min}}) = 0$. The budding process is assumed to proceed with no effect on the coronal blocks; i.e., $N_B^{1/3}a \ll L$. This, of course, is not strictly true. The budding process is always associated with some displacement of the coronal block. The outward shift of the A block results in loss of free energy. This in turn leads to a smaller F^* and y^*. However, as the correction to F^* is expected to be small and as y^* does not play a crucial role in our considerations, both effects may be ignored. For similar reasons, the budding process may modify the coronal contribution to $F(y)$. This modification is not important because when the effect is nonnegligible, it turns out to have a marginal effect on the expulsion rate constant. In the same spirit, we now assume that the expulsion of the coronal block takes place with no effect on the collapsed B block. Thus, for $y^* \leq y \leq R_{\text{core}} + L$, we have

$$F(y) = F^* + \Delta\Phi_{\text{corona}}(y) \qquad \text{(IV-8)}$$

where $F^* \approx \gamma a^2 N_B^{2/3}$ and $\Delta\Phi_{\text{corona}}(y)$, the change in the free energy of the whole corona as a function of the expulsion progress is given by

$$\Delta\Phi_{\text{corona}}/kT = \Phi_{\text{corona}}(y)/kT - \Phi_{\text{corona}}(y^*)/kT \approx f^{3/2} \ln \frac{R_{\text{core}} + L}{y} + (f-1)^{3/2} \ln \frac{y}{R_{\text{core}}} - f^{3/2} \ln \frac{R_{\text{core}} + L}{R_{\text{core}}} \approx -f^{1/2}\left(\ln \frac{R_{\text{core}} + L}{R_{\text{core}}} - \ln \frac{R_{\text{core}} + L}{y} \right) \qquad \text{(IV-9)}$$

To obtain $\Delta\Phi_{\text{corona}}$ we assume that in the two spherical shells, $y^* < r < y$ and $y < r < R_{\text{core}} + L$, the coronal chains assume the equilibrium structure appropriate to spherical grafted layers consisting respectively of $f - 1$ and f grafted chains. Note, that for large f's, $\Delta\Phi_{\text{corona}}$ is essentially due to the change in the free energy of the expelled coil.

The implementation of the Kramers theory does not require the detailed free-energy profile. The necessary input consists of two characteristic parameters: the height of the barrier, F^*; and the barrier's width, α. The definition of F^* is straightforward, but the identification of the true α is more delicate. For the budding process, the interval $F^* - kT$ to F^* is associated with a miniscule change in y, ϵ, determined by the condition

$$\gamma a^2[N_B^{2/3} - (N_B^{1/3}a - \epsilon)^2/a^2] \approx kT \qquad \text{(IV-10)}$$

For $\gamma a^2 \approx kT$ and $\epsilon \ll N_B^{1/3}a$, we obtain

$$N_B^{2/3}[1 - (1 - \epsilon/N_B^{1/3}a)^2] \approx \epsilon N_B^{1/3}a^{-1} \approx 1 \qquad \text{(IV-11)}$$

or $\epsilon \approx N_B^{-1/3}a$. This, however, is not the relevant α. The relevant α is the curvilinear length of the embedded B block for $F^* - kT$, given by $\alpha/a \approx a^{-3}\epsilon N_B^{2/3}a^2 \approx N_B^{1/3}$. This choice accounts for the mechanism responsible for the bud growth that is the transfer of the final embedded B segment from the core onto the bud. This must be supplemented by the coronal contribution which is equal to the size of the innermost blob, i.e., $\xi(R_{\text{core}} + 2N_B^{1/3}a)$. Altogether we have

$$\alpha \approx 2N_B^{1/3}a + \xi(R_{\text{core}} + 2N_B^{1/3}a) \qquad \text{(IV-12)}$$

because $\xi \sim r$, we have $\xi(R_{\text{core}} + 2N_B^{1/2}a) \approx \xi(R_{\text{core}})(R_{\text{core}} + 2N_B^{1/3}a)/R_{\text{core}} \sim \xi(R_{\text{core}})(f^{1/3} + 2)/f^{1/3} \sim \xi(R_{\text{core}})$ and $\xi^2(R_{\text{core}}) \sim R_{\text{core}}^2/f$ or $\xi(R_{\text{core}}) \approx f^{-1/6}N_B^{1/3}a$. Equation IV-12 is, however, misleading because each of the two terms is associated with a different diffusion coefficient. We picture the motion of the embedded B segment as decoupled from that of the already expelled B block. Accordingly, the associated diffusion time, τ_B, is roughly the time needed by the embedded segment to diffuse its own length. As

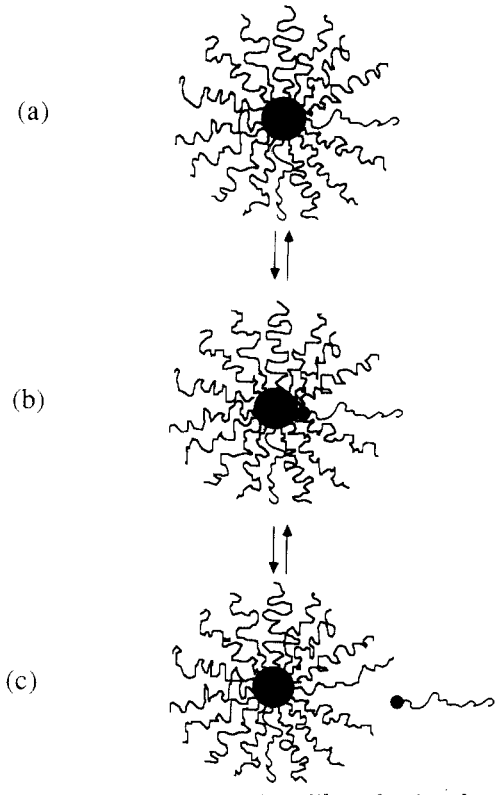

Figure 5. Elementary step in the AW mechanism for starlike micelles: (a) corresponds to the well's minimum; (b) to the reactive intermediate, y^*; and (c) to the final stage, y_{bulk}.

the corresponding D scales as $N_B^{-1/3}$, we obtain $\tau_B \sim N_B$. The coronal contribution to $\tau_{barrier}$ is due to diffusion across a distance of $\xi(R_{core})$. In this case, the frictional interactions are due primarily to the A block. Assuming that each blob acts as a hydrodynamically impenetrable sphere,[27] we have $D \sim L^{-1}$ and the diffusion time τ_A scales as $\tau_A \sim D^{-1}\xi^2$. As we focus on the scaling behavior of $\tau_1, f = \langle f \rangle$ as given by (II-8) while L is given by (III-3). Accordingly $\xi(R_{core})$ scales as $N_B^{1/6}$ for micelles with thin coronas and as $N_B^{1/5}$ for starlike micelles. Therefore $\tau_{barrier}$ is

$$\tau_{barrier} = \tau_B + \tau_A \sim \begin{cases} N_B + N_A N_B^{2/9} \approx N_B & N_A \ll N_B \\ N_B + N_A^{3/5} N_B^{14/25} \approx N_A^{3/5} N_B^{14/25} & N_A \gg N_B \end{cases} \quad \text{(IV-13)}$$

and $\upsilon_{barrier}$ is thus

$$\upsilon_{barrier} \approx \begin{cases} N_B^{1/3} a/\tau_B \sim N_B^{-2/3} & N_A \ll N_B \\ \xi(R_{core})/\tau_A \sim N_A^{-3/5} N_B^{-9/25} & N_A \gg N_B \end{cases} \quad \text{(IV-14)}$$

The Kramers theory is based on the identification of $\tau_{barrier}$ as the lifetime of the reactive intermediate, i.e., the passage from $y^* + \alpha/2$ into the bulk is assumed to take place on a much shorter time scale. This assumption is justified when the free-energy barrier is sharply peaked at y^*. For polymeric micelles, this is not always the case: while the barrier is always steep when approached from the well's minimum, the outer slope can be both mild and of very long range (Figure 4). Such is the case for starlike micelles. Thus, while our analysis so far yields the correct J for micelles with thin coronas, the expulsion dynamics in starlike micelles must account for the effect of the corona (Figure 5). The exterior, coronal segment of the potential barrier is given by (IV-9). For starlike micelles, where $L \gg R_{core}$, $\langle f \rangle \sim N_B^{4/5}$, and $L \sim N_B^{4/25} N_A^{3/5} a$, the coronal contribution to $F(y)$ is given by

$$F(y)/kT \approx -f^{1/2}\left(\ln \frac{L}{R_{core}} - \ln \frac{L}{y}\right) \approx -N_B^{4/10}(\ln N_B^{-11/25} N_A^{3/5} - \ln N_B^{4/25} N_A^{3/5} a/y) \quad R_{core} < y \le R_{core} + L \quad \text{(IV-15)}$$

a potential which is both long ranged and slowly varying (logarithmic in y). This $F(y)$ may be regarded as originating from gradual release from confinement. As noted in section II, each coronal chain is in effect grafted to the narrow end of a truncated cone. $F(y)$ is the free energy of a chain which is partly expelled from such a cone, measured with respect to that of a fully confined coil. A related, and crucial, observation is that the coronal chains are stretched: L is equal to the sum of blob diameters. Note that while globally the coil is only weakly stretched, it is strongly stretched when viewed as a chain of blobs. The chain's stretched configuration suggests reptation-type dynamics[28,29] because a shift in the chain center of gravity is obtained by a curvilinear displacement along the chain's contour.

It is convenient to describe the passage through the corona by means of the Langevin equation[29] for the diblock copolymer coil:[16]

$$\frac{dy}{dt} = -\frac{1}{\zeta(y)} \frac{\partial F(y)}{\partial y} + \frac{1}{\zeta_{chain}} f(t) \quad \text{(IV-16)}$$

where $f(t)$ is assumed to be a Gaussian random force characterized by the moments $\langle f(t) \rangle = 0$ and $\langle f(t) f(t') \rangle = 2\zeta_{chain} kT \delta(t - t')$. The first LHS terms describe the effect of the nonrandom force on the embedded segment. For $F(y)$ given by (IV-15), the outward directed force, $-\partial F(y)/\partial y$, is equal to $kTf^{1/2}y^{-1}$. The associated frictional term, $\zeta^{-1}(y)$, must account for the contribution of the embedded monomers only. The second term relates to the effects of random forces on the entire chain. Accordingly, the corresponding frictional term, ζ_{chain}, accounts for the contribution of all monomers in the coil. Assuming as before that blobs behave hydrodynamically as impenetrable spheres,[27,30] we immediately find $\zeta(y) \sim 6\pi\eta_3(L - y)$, while $\zeta_{chain} \sim \zeta(y) + \zeta_{ex}$, where $\zeta_{ex} \sim 6\pi\eta_s N_{ex}^{3/5} a$ is the contribution of the N_{ex} for the already expelled A monomers. Note that the frictional forces during the coronal passage are assumed to arise only because of solvent viscosity, η_s. Equation IV-16 allows us to calculate the probability density, Φ, for finding the A–B junction at a position y. Φ is peaked at $\langle y(t) \rangle$. The nonrandom force causes a shift in $\langle y(t) \rangle$, while the random forces lead to widening of Φ. Both processes may lead to chain expulsion. A rough estimate of τ_{corona} may be obtained by solving (IV-16) when one of the terms is dominant. The purely diffusive τ_{corona} is obtainable by using $L^2 \sim D\tau_{corona}$. Because $\xi(y)$ is position dependent, an effective D is required. It is simpler, however, to consider bounds on D and thus on the associated τ_{corona}. Clearly, $kT/6\pi\eta_s L \le D = kT/\zeta_{chain} \le kT/6\pi\eta_s N_A^{3/5} a$, leading to $(kT/6\pi\eta_s a^3) N_B^{8/25} N_A^{9/5} \le \tau_{corona} \le (kT/6\pi\eta_s a^3) N_B^{12/25} N_A^{9/5}$. When the nonrandom force is dominant, (IV-16) reduces to $dy/dt \sim (kT/6\pi\eta_s) f^{1/2}/y(L - y)$, which leads to

$$\tau_{corona} \sim L^3 f^{-1/2}(6\pi\eta_s/kT) \sim N_B^{2/25} N_A^{9/5} \quad \text{(IV-17)}$$

and

$$\upsilon_{corona} \sim L/\tau_{corona} \sim L^{-2} f^{1/2} \sim N_B^{2/25} N_A^{-6/5} \quad \text{(IV-18)}$$

For starlike micelles, for which $N_A \gg N_B$, the nonrandom τ_{corona} is both shorter than the diffusive τ_{corona} and much

longer than $\tau_{barrier}$. Furthermore, v_{corona} is slower than $v_{barrier}$. We thus identify τ_{corona} as the intermediate's lifetime for starlike micelles. For such micelles, J and thus b are determined by (IV-17) and (IV-18) rather than (I-V-13) and (IV-14). Using these results as well as (IV-4) and (IV-5), we find

$$b \sim \begin{cases} \exp(-F^*/kT)v_{barrier}/R_{core} \sim \exp(-N_B^{2/3}\gamma a/kT)N_B^{-4/3} & N_A \ll N_B \\ \exp(-F^*/kT)v_{corona}/L \sim \exp(-N_B^{2/3}\gamma a^2/kT)N_B^{-2/25}N_A^{-9/5} & N_A \gg N_B \end{cases} \quad \text{(IV-19)}$$

This finally allows us to write down the scaling forms of τ_1 for micelles with thin coronas and for starlike micelles

$$\frac{1}{\tau_1} \sim \begin{cases} \exp(-N_B^{2/3}\gamma a^2/kT)N_B^{-2}(1 + N_B^{-1/3}X) & N_A \ll N_B \\ \exp(-N_B^{2/3}\gamma a^2/kT)N_B^{-12/25}N_A^{-9/5}(1 + N_B^{-2/5}X) & N_A \gg N_B \end{cases} \quad \text{(IV-20)}$$

While τ_1 of micelles with thin coronas ($N_A \ll N_B$) depends only on B_B, τ_1 of starlike micelles ($N_A \gg N_B$) scales as $N_A^{9/5}$. The N_A dependence is solely due to the expulsion rate constant, b. Thus, by varying N_A it is possible to modify τ_1 by changing b and with little effect on the equilibrium characteristics of the micellar solution.

V. Discussion

The first prediction of this paper concerns the relaxation mechanism of polymeric micelles. Our considerations suggest that the Aniansson–Wall mechanism is dominant for micelles formed by diblock copolymers in a selective low molecular weight solvent. While our discussion focused on two extreme micellar types, endowed with thin or extended coronas, we expect this prediction to hold for intermediate cases as well. Accordingly, the slow relaxation time, τ_2, of such solutions is expected to increase with micellar concentration (eq III-18) rather than decrease, as predicted for the fission–fusion mechanism. Note that the fast relaxation time, τ_1, is usually determined by the AW mechanism and thus cannot be used to test this prediction.

The second result concerns the scaling behavior of the expulsion rate constant b and of the fast relaxation time $\tau_1 \sim b^{-1}$. We find that the exponential factor in both τ_1 and b is determined solely by the size of the core B block. On the other hand, the preexponential factor is determined solely by the B block only for micelles with thin coronas. The preexponential factor in b of starlike micelles is traceable to the passage through the corona and is thus strongly dependent on the coronal block DP. This last feature allows us to modify the rate constant with no accompanying change in the solution's equilibrium characteristics which are determined primarily by the B block. Accordingly, τ_1 of starlike micelles may allow us to probe the dynamics of expulsion through the corona. These are of interest because they exhibit features which are specific to grafted chains: (i) because the chains are stretched, the motion is reptative in nature even in the absence of entanglements; (ii) the outward motion is driven, albeit weakly, by free-energy gradient due to gradual release from confinement during the expulsion.

The expulsion rate constant, b, was analyzed in the framework of the Kramers rate theory. The macromolecular nature of our system gives rise to special, polymeric modifications of this theory: (i) The displacement along the reaction coordinate is sometimes much shorter than the actual path traversed by the chain segments. This effect, which is reminiscent of reptation, is important in determining the time scales of the process. (ii) For starlike micelles, the intermediate's lifetime is determined by the external tail of the potential rather than by the vicinity of the saddle point. This effect is due to the self-consistent potential acting on the coils which is produced by all other micellar chains. Thus, by increasing the size of the coronal blocks, we can change the range of the potential tail to the point where the system spends more time in this region than in the vicinity of the saddle point.

Our analysis was based on scaling arguments and is thus best suited to large N_A and N_B. However, as τ_1 grows exponentially with $N_B^{2/3}$, the use of micelles formed by diblock copolymers with large B blocks may prove impractical. It would seem that starlike micelles provide the most convenient experimental system from this point of view. Also it is important to operate above the glass transition temperature, T_g, of the core blocks. Below this T_g, which may well differ from the bulk value, the solution might exhibit irreproducible relaxation behavior.[31] Finally, while our analysis was carried out with various relaxation experiments—T jump, etc.—in mind, other related methods may be used to test our predictions concerning the expulsion rate constant, b. As b determines the residence time of a diblock copolymer coil in a micelle,[14] it should be possible to use time-resolved fluorescence quenching[1,28] to investigate its scaling behavior.

Acknowledgment. The authors were initiated into this field by a series of lectures by R. Zana in UCSB in August 1987. It is a pleasure to acknowledge useful discussions with W. T. Tang. This work was supported by the U. S.-Israel Binational Science Foundation (BSF) Jerusalem, Israel, and in part by the Department of Energy under Grant DE-FG03-87ER45288. The Fritz Haber Research Center is supported by the Minerva Gesellschaft für die Forschung, mbH, Munich, BRD.

References and Notes

(1) Zana, R. In *Surfactants in Solution*; Mittal, K. L., Bothorel, P., Eds.; Plenum Press: New York, 1986; Vol. 4.
(2) Kahlweit, M. In *Physics of Amphiphiles, Micelles, Vesicles and Microemulsions*; Degiorgio, V., Corti, M., Eds.; North Holland: Amsterdam, 1985.
(3) (a) Price, C. In *Developments in Block Copolymers*; Goodman, I., Ed.; Applied Science: New York, 1982; Vol. 1. (b) Price, C. *Pure Appl. Chem.* **1983**, *55*, 1563. (c) Tang, W. T., unpublished results. This experimental work is concerned with exchange kinetics between micelles formed by triblock copolymers.
(4) Tuzar, Z.; Kartochvil, P. *Adv. Colloid Interface Sci.* **1976**, *6*, 201.
(5) de Gennes, P.-G. In *Solid State Physics*; Liebert, L., Ed.; Academic Press: New York, 1978; Suppl. 14.
(6) (a) Noolandi, J.; Hong, K. M. *Macromolecules* **1985**, *15*, 482. (b) Noolandi, J.; Hong, K. M. *Macromolecules* **1983**, *16*, 1443. (c) Whitmore, M. D.; Noolandi, J. *Macromolecules* **1985**, *18*, 657.
(7) Leibler, L.; Orland, H.; Wheeler, J. C. *J. Chem. Phys.* **1983**, *79*, 3550.
(8) ten Brinke, G.; Hadziioannou, G. *Macromolecules* **1987**, *20*, 486.
(9) Bug, A. L. R.; Cates, M. E.; Safran, S. A.; Witten, T. A. *J. Chem. Phys.* **1987**, *87*, 1824.
(10) Halperin, A. *Macromolecules* **1987**, *20*, 2943.
(11) Marques, C.; Joanny, J. F.; Leibler, L. *Macromolecules* **1988**, *21*, 1051.
(12) Aniansson, E. A. G.; Wall, S. N. *J. Phys. Chem.* **1972**, *78*, 1024; **1975**, *79*, 986.

(13) Aniansson, E. A. G.; Wall, S. N.; Almgren, M.; Hoffman, H.; Kielmann, I.; Ulbricht, W.; Zana, R.; Lang, J.; Tondre, C. *J. Phys. Chem.* **1976**, *80*, 905.
(14) Kahlweit, M. *J. Colloid Interface Sci.* **1982**, *90*, 92.
(15) Witten, T. A.; Pincus, P. A. *Macromolecules* **1986**, *19*, 2509.
(16) Halperin, A.; Alexander, S. *Europhys. Lett.* **1988**, *6*, 329.
(17) Halperin, A. *Europhys. Lett.*, in press.
(18) Semenov, A. N. *Sov. Phys.—JETP (Engl. Transl.)* **1985**, *61*, 733.
(19) Daoud, M.; Cotton, J. P. *J. Phys. (Les Ulis, Fr.)* **1982**, *43*, 531.
(20) Alexander, S. *J. Phys. (Les Ulis, Fr.)* **1977**, *38*, 983.
(21) de Gennes, P.-G. *Macromolecules* **1980**, *13*, 1069.
(22) (a) Milner, S. T.; Witten, T. A.; Cates, M. *Europhys. Lett.* **1988**, *5*, 413. (b) Milner, S. T.; Witten, T. A.; Cates, M. *Macromolecules* **1988**, *21*, 2610.
(23) Leibler, M.; Pincus, P. A. *Macromolecules* **1984**, *17*, 2922.
(24) Glasstone, S.; Laidler, K. J.; Eyring, H. *The Theory of Rate Processes*; McGraw-Hill: New York, 1941.
(25) (a) Kramers, H. A. *Physica (Amsterdam)* **1940**, *7*, 284. (b) Chandrasekhar, S. *Rev. Mod. Phys.* **1943**, *15*, 1.
(26) For recent reviews, see: (a) Nitzan, A. *Adv. Chem. Phys.* **1988**, *70*, 489. (b) Hanggi, P. *J. Stat. Phys.* **1986**, *42*, 105.
(27) (a) Brochard, F.; de Gennes, P.-G. *Macromolecules* **1977**, *10*, 1157. (b) Brochard, F. *J. Phys. (Les Ulis, Fr.)* **1983**, *44*, 39.
(28) de Gennes, P.-G. *Scaling Concepts in Polymer Physics*; Cornell University Press: Ithaca, NY, 1979.
(29) Doi, M.; Edwards, S. F. *The Theory of Polymer Dynamics*; Oxford University Press: New York, 1986.
(30) In ref 16, the blobs were considered to be free draining.
(31) Kremer, K. *J. Phys. (Les Ulis, Fr.)* **1983**, *47*, 1269.

Flexible Polymer with Excluded Volume at an Interacting Penetrable Surface of Variable Dimension: A Multiple-ϵ Perturbation Theory

Jack F. Douglas*

Polymers Division, National Bureau of Standards, Gaithersburg, Maryland 20899

Marios K. Kosmas

Chemistry Department, University of Ioannina, Ioannina, Greece. *Received April 1, 1988*

ABSTRACT: Application of the renormalization group method to the perturbative treatment of surface interacting polymers with excluded volume currently requires the surface dimension to be fixed. A multiple-ϵ perturbation expansion method is proposed to circumvent this technical restriction. There are numerous potential applications of multiple-ϵ perturbation theory (e.g., combined treatment of binary and ternary excluded volume interactions) which can be pursued once the internal consistency of the method is demonstrated in higher order calculations. The surface interaction model provides a good starting point for studying the multiple-ϵ method because of the relative simplicity of the perturbative calculations that provide the input into the multiple-ϵ renormalization group calculations. Another convenient aspect of the model is that the consistency of the multiple-ϵ method can be checked against accurate results for the limits of each interaction (surface and excluded volume) alone and the combined interactions for the special case of a two-dimensional surface.

1. Introduction

The theoretical description of isolated polymers in the presence of an interacting boundary has been considered by using both lattice random walk and continuum Gaussian chain models. Rubin[1] and Hammersley[2] studied random walks interacting with surfaces of varying dimension $d_\parallel$ (point, $d_\parallel = 0$; line, $d_\parallel = 1$; etc.) and calculated many of the important configurational properties of ideal polymers with no polymer–polymer interactions. There are complementary studies for the continuum model formulation of surface ($d_\parallel = 2$) interacting Gaussian chains at an impenetrable surface,[3] and numerous calculations address the problem of surface interacting chains with excluded volume[4-9] (see below).

Recent calculations by Kosmas[6] and Douglas et al.[7] consider the problem of a surface interacting chain from the general perspective where the interacting surface is taken to have a continuously variable dimension. Initial calculations by Kosmas[6] introduced the model and utilized a version of the renormalization group (RG) theory to calculate certain exponents characterizing the number of polymer configurations subject to the surface constraint. More recent calculations by Douglas et al.[7] give *exact* calculations for many configurational properties over the full range (attractive and repulsive) of surface interactions, which they then compare with the corresponding scaling functions obtained using the approximate Gell-Mann–Low RG theory. Those calculations enable the unambiguous estimation of ϵ-expansion errors in the scaling functions order by order in ϵ perturbation theory and are also useful for understanding the characteristic failure of the RG theory to describe polymers with attractive polymer–polymer or polymer–surface interactions.[7]

Both Kosmas[6] and Douglas et al.[7] have applied the RG schemes to treat the combined influence of polymer excluded volume and surface interactions for the special case where the surface dimension is fixed at two dimensions so that the ϵ-expansion method can be applied to both interactions. Kosmas' calculation[6] emphasizes the combined effect of surface and excluded volume interactions on the exponents that characterize the number of chain configurations, while the work of Douglas et al.[7] describes the effect of excluded volume on the scaling functions of configurational properties such as the end vector distance $\langle \mathbf{R}^2 \rangle$ in relation to the properties calculated without excluded volume. Of course, the combined treatment of polymer excluded volume and surface interactions necessarily becomes approximate once excluded volume is incorporated into the theory and is then primarily restricted to repulsive polymer–polymer and polymer–surface interactions.

Despite the extensive work that has been done on surface interacting chains, there are numerous important problems that remain. For example, the effect of surface proximity[8] of a particular chain to the surface, polymer confinement to a finite region with interacting boundaries,[8]

0024-9297/89/2222-2412$01.50/0